



Test Platform for Advanced Digital Control of Brushless DC Motors

(MSFC Center Director's Discretionary Fund Final Report,
Project No. 00-04)

D.A. Gwaltney

Marshall Space Flight Center, Marshall Space Flight Center, Alabama



The NASA STI Program Office...in Profile

Since its founding, NASA has been dedicated to the advancement of aeronautics and space science. The NASA Scientific and Technical Information (STI) Program Office plays a key part in helping NASA maintain this important role.

The NASA STI Program Office is operated by Langley Research Center, the lead center for NASA's scientific and technical information. The NASA STI Program Office provides access to the NASA STI Database, the largest collection of aeronautical and space science STI in the world. The Program Office is also NASA's institutional mechanism for disseminating the results of its research and development activities. These results are published by NASA in the NASA STI Report Series, which includes the following report types:

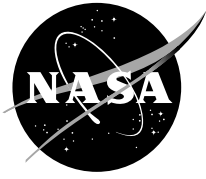
- **TECHNICAL PUBLICATION.** Reports of completed research or a major significant phase of research that present the results of NASA programs and include extensive data or theoretical analysis. Includes compilations of significant scientific and technical data and information deemed to be of continuing reference value. NASA's counterpart of peer-reviewed formal professional papers but has less stringent limitations on manuscript length and extent of graphic presentations.
- **TECHNICAL MEMORANDUM.** Scientific and technical findings that are preliminary or of specialized interest, e.g., quick release reports, working papers, and bibliographies that contain minimal annotation. Does not contain extensive analysis.
- **CONTRACTOR REPORT.** Scientific and technical findings by NASA-sponsored contractors and grantees.

- **CONFERENCE PUBLICATION.** Collected papers from scientific and technical conferences, symposia, seminars, or other meetings sponsored or cosponsored by NASA.
- **SPECIAL PUBLICATION.** Scientific, technical, or historical information from NASA programs, projects, and mission, often concerned with subjects having substantial public interest.
- **TECHNICAL TRANSLATION.**
English-language translations of foreign scientific and technical material pertinent to NASA's mission.

Specialized services that complement the STI Program Office's diverse offerings include creating custom thesauri, building customized databases, organizing and publishing research results...even providing videos.

For more information about the NASA STI Program Office, see the following:

- Access the NASA STI Program Home Page at [*http://www.sti.nasa.gov*](http://www.sti.nasa.gov)
- E-mail your question via the Internet to [*help@sti.nasa.gov*](mailto:help@sti.nasa.gov)
- Fax your question to the NASA Access Help Desk at (301) 621-0134
- Telephone the NASA Access Help Desk at (301) 621-0390
- Write to:
NASA Access Help Desk
NASA Center for AeroSpace Information
7121 Standard Drive
Hanover, MD 21076-1320



Test Platform for Advanced Digital Control of Brushless DC Motors

**(MSFC Center Director's Discretionary Fund Final Report,
Project No. 00–04)**

D.A. Gwaltney

Marshall Space Flight Center, Marshall Space Flight Center, Alabama

National Aeronautics and
Space Administration

Marshall Space Flight Center • MSFC, Alabama 35812

Available from:

NASA Center for AeroSpace Information
7121 Standard Drive
Hanover, MD 21076-1320
(301) 621-0390

National Technical Information Service
5285 Port Royal Road
Springfield, VA 22161
(703) 487-4650

TABLE OF CONTENTS

1. INTRODUCTION	1
2. BACKGROUND	2
3. APPROACH	3
4. CONTROLLERS	5
4.1 Proportional-Integral-Derivative Controller	5
4.2 Adaptive Exact Model Knowledge Controller	5
4.3 Self-Tuning Controller	6
5. EXPERIMENTS	8
5.1 Comparison of Proportional-Integral-Derivative and Adaptive Exact Model Knowledge Controller	8
5.2 Comparison of Pole Placement and Self-Tuning Controllers	14
6. SUMMARY	17
REFERENCES	19

LIST OF FIGURES

1.	Brushless DC motor control experimental configuration	3
2.	DSP controller card	4
3.	PID controller response with 27-lb load for (a) position, (b) error, and (c) input.....	8
4.	PID controller response with 50-lb load for (a) position, (b) error, and (c) input.....	9
5.	Adaptive EMK controller error response with (a) 27-lb load and (b) 50-lb load	10
6.	Parameters estimated by the adaptive EMK controller for 27-lb load for (a) inertia, (b) damping, and (c) load torque	11
7.	Parameters estimated by the adaptive EMK controller for 50-lb load for (a) inertia, (b) damping, and (c) load torque	12
8.	Adaptive EMK control input to the translation stage with 50-lb load	13
9.	Online estimation of system parameters by STC for (a) a_1 and a_2 and (b) b_0	14
10.	STC performance with 27-lb load for (a) position response to desired position trajectory, (b) error, and (c) input	15
11.	Comparison of STC and standard pole placement control for (a) position response and (b) error	16

LIST OF TABLES

1.	PID control tracking error metrics	9
2.	Adaptive EMK control tracking error metrics	11

LIST OF ACRONYMS

BLDC	brushless DC
DSP	digital signal processor
EMA	electromechanical actuator
EMK	exact model knowledge
MSFC	Marshall Space Flight Center
PCB	printed circuit board
PD	proportional derivative
PID	proportional-integral-derivative
STC	self-tuning controller
VME	Versa Module Eurocard

NOMENCLATURE

a_1	parameter
a_2	parameter
B	damping
b_0	parameter
b_1	parameter
e	error
J	inertia
K_D	derivative gain
K_I	integral gain
K_P	proportional gain
K_S	control gain
$K_{\tau 2}$	current to torque conversion factor
k	index for the k th sample time
q	position of the stage carriage
q_D	desired position trajectory
s	complex variable for Laplace transforms
T	sampling period; z -transformed polynomial
T_E	applied torque
T_L	load torque
t	time
u	control input
u_c	desired trajectory
y	system output
z	complex variable for z -transforms
α	control gain
β	arbitrary gain factor
ω	rotational speed of the motor shaft

TECHNICAL MEMORANDUM

TEST PLATFORM FOR ADVANCED DIGITAL CONTROL OF BRUSHLESS DC MOTORS (MSFC Center Director's Discretionary Fund Final Report, Project No. 00-04)

1. INTRODUCTION

The goal of this effort is to develop a test platform for development, implementation, and evaluation of adaptive and other advanced control techniques for brushless DC (BLDC) motors used in translation and positioning systems. The test platform will be used to test and select control techniques for BLDC motor-driven systems for various applications. The control approach to be evaluated will be implemented as a digital control algorithm in an embedded digital control processor. Important applications for a BLDC motor-driven system are the translation of specimens in microgravity experiments and electromechanical actuation of nozzle and fuel valves in propulsion systems. Motor-driven aerocontrol surfaces are also being utilized in developmental X vehicles. The performance of advanced control approaches will be compared with the performance of linear controllers with fixed control gains. This effort includes the design and fabrication of a printed circuit board (PCB) using a digital signal processor (DSP) device suitable for the implementation of an advanced controller. This PCB has a small form factor and will serve as the main processing unit for digital control algorithms. The controller PCB will interface to appropriate electronics for driving the BLDC motor and signal conditioning electronics for measured signals used as feedback. This will allow peripheral electronics to be chosen to suit a wide variety of applications. This effort will provide hardware and reusable algorithms for application to future space vehicles and spaceborne experiments. This effort provides the implementation of control approaches for BLDC motor-driven actuators with improved performance in the face of unanticipated changes in the dynamics of the mechanical systems due to normal wear and tear, and for operation outside expected load conditions.

2. BACKGROUND

Embedded control of BLDC motor-driven systems is currently being used in the design of propulsion systems and microgravity experiments at Marshall Space Flight Center. Some of the electro-mechanical actuators (EMAs) developed for use in nozzle and fuel valve positioning are BLDC motor-based designs. Many microgravity experiments employ BLDC motor-driven linear stages for specimen or camera translation. In general, these embedded control designs employ linear proportional-integral-derivative (PID) control. This is an attractive approach because it does not require a theoretical model of the system and is a proven method of control. To give some perspective, the Ziegler-Nichols tuning method for PID controllers was developed in the 1940s. When project deadlines are on the horizon, the tried-and-proven approach is often the one taken. In practice, the selection of gains for a PID controller is largely ad hoc and subject to the trial-and-error method of refinement. This means that while the PID control works, it is not necessarily the best control approach available. It is true that PID control can be enhanced using gain scheduling over a range of known operating conditions, but this requires knowledge that may be inaccurate or subject to change over time. There are many advanced control approaches that can be used to provide higher accuracy and more robust response to unexpected changes or nonlinear characteristics in the mechanical system being controlled. Additionally, the latest generation of low-power DSP devices and supporting electronics can further reduce the power needed to operate the control system.

3. APPROACH

This effort is based on analyzing existing controller designs developed for microgravity experiments. A new DSP processor PCB design is produced using recently released, faster and lower power DSP devices. The new design is focused on providing a flexible embedded controller PCB, while the existing designs are application specific. A general test platform is implemented that consists of a computer to compile and download the control algorithm code to the DSP on the controller card. The computer is used to debug the code and to provide performance data storage and analysis. The controller card acquires feedback signals from position and velocity sensors through appropriate signal conditioning circuitry and provides command signals to the motor driver for a BLDC motor-driven system. A diagram of the system is shown in figure 1. The experimental mechanical system is a translation stage that will move a variable load vertically with respect to gravity. In this effort, the implementation and testing of adaptive control algorithms is done using the prototype DSP controller board. Experiments are conducted to verify improvements in system performance obtained using the adaptive control algorithms. These experiments are executed using linear algorithms and the adaptive control algorithms on the same hardware. The response of the linear and advanced control algorithms will be recorded with varying loads on the translation stage. Performance is evaluated by collecting data and comparing system response under different control approaches.

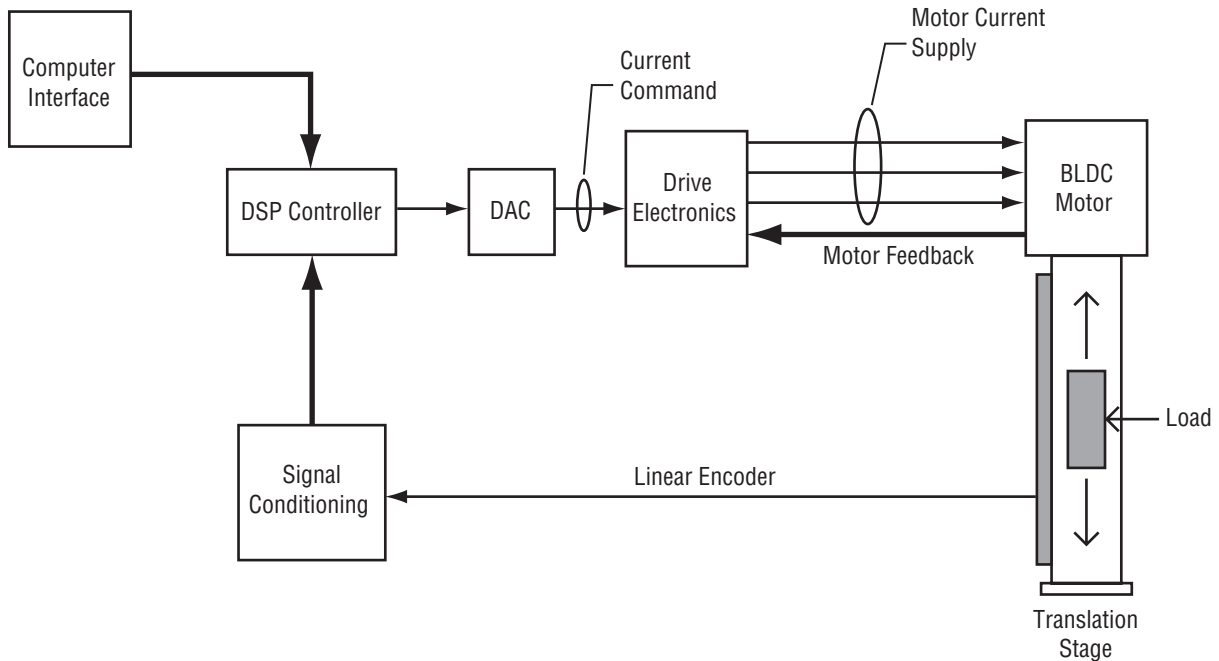


Figure 1. Brushless DC motor control experimental configuration.

The DSP controller is pictured in figure 2. The PCB form factor is a single-height Versa Module Eurocard (VME) board with dimensions of 3.937 in by 6.299 in. A 96-pin VME backplane connector is used, but the pin definitions are customized and do not follow the VME specification. This connector is used to route signals between the controller card and the signal conditioning cards required to control the motor-driven translation stage.

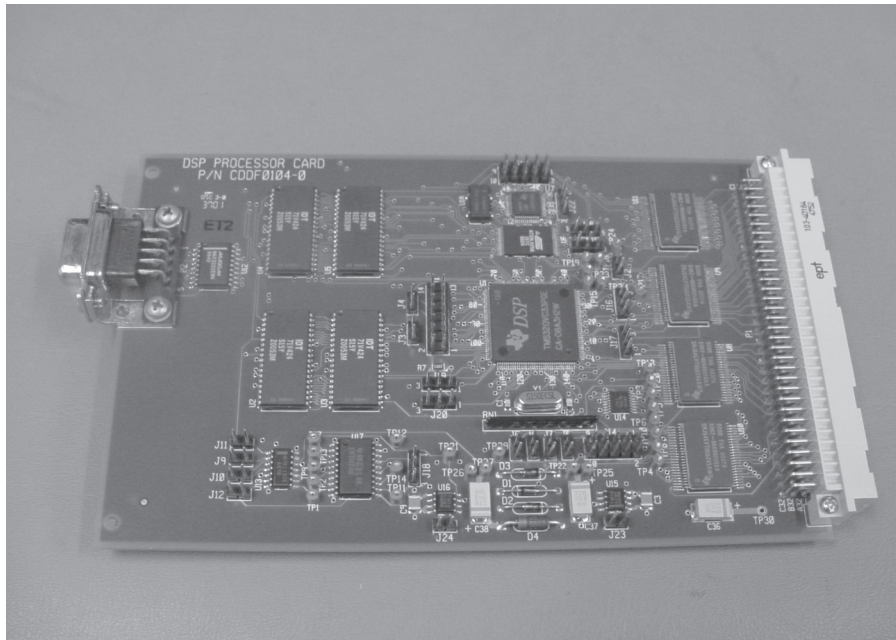


Figure 2. DSP controller card.

4. CONTROLLERS

4.1 Proportional-Integral-Derivative Controller

The linear PID control algorithm code is written in C and implemented as firmware on the DSP controller card. A linear PID controller in continuous time has the following form:

$$u(t) = K_P e(t) + \frac{1}{K_I} \int e(t) dt + K_D \frac{de(t)}{dt} , \quad (1)$$

where

- u = output of the controller and the input to the controlled system
- e = error and is defined as e = desired trajectory – stage carriage position
- K_P = proportional gain
- K_I = integral gain
- K_D = derivative gain.

For implementation in a discrete time control system, the continuous time equations are converted to a difference equation form:

$$u(k) = K_P e(k) + \frac{T}{K_I} S(k) + K_D \frac{e(k) - e(k-1)}{T} ,$$
$$S(k) = S(k-1) + e(k) , \quad (2)$$

where

- T = sampling period
- k = index for the k th sample time
- S = sum of the error values at the k th sample time.

The error and controller gain definitions are the same as for equation (1).

4.2 Adaptive Exact Model Knowledge Controller

In this investigation, a commercial motor drive is used that accepts a torque (current) command input and produces the commanded torque at the output of the motor shaft. This inner torque control loop allows the controller implemented in firmware on the DSP controller card to command motor

torque. To the controller, the system dynamics of the motor-driven stage are represented by the following equation:

$$T_E(t) = J\dot{\omega}(t) + B\omega(t) + T_L, \quad (3)$$

where

T_E = torque input to the system produced by the motor
 J = inertia in the system
 B = damping in the system
 T_L = load torque
 ω = rotational speed of the motor shaft.

This equation is used in an exact model knowledge (EMK) controller¹ to produce command input based on knowledge of system dynamics. The controller combines a linear proportional-derivative (PD) controller with terms based on the system dynamics equation. The continuous time controller is defined by the following equation

$$u(t) = K_{\tau 2} \left[K_S (\dot{e}(t) + \alpha e(t)) \right] + J (\ddot{q}_D(t) + \alpha \dot{e}(t)) + B \dot{q}(t) + T_L, \quad (4)$$

where

$K_{\tau 2}$ = current to torque conversion factor
 K_S = positive control gain
 α = positive control gain
 e = error and is defined as $e = q_D - q$
 q_D = desired position trajectory (mm)
 q = position of the stage carriage (mm).

In the EMK controller, K_S and α can be related to K_P and K_D in a linear PD controller. For implementation in a discrete time control system, the second derivative of the desired trajectory, the first derivative of the stage carriage position, and the derivative of the error are calculated using approximations. For adaptive control, the inertia, damping, and load torque of the system are estimated online. The interested reader is referred to Dawson et al.¹ for the derivation of the adaptation approach.

4.3 Self-Tuning Controller

Another approach to adaptive control is the implementation of a self-tuning controller (STC).² Astrom and Wittenmark refer to these controllers as self-tuning regulators, but regulation implies rejection of disturbances to maintain a process at a constant setpoint, while control implies the broader action of following a desired trajectory and rejecting disturbances. The term “controller” is therefore used in this Technical Memorandum rather than “regulator.” The STC implementation uses pole placement control design in conjunction with parameter estimation to provide a controller that can calculate its own control gains online. A general discrete-time linear controller can be described by

$$R(z)u(z) = T(z)u_c(z) - S(z)y(z) , \quad (5)$$

where R , T , and S are z -transformed polynomials. In equation (5), $u(z)$ is the control input, $u_c(z)$ is the desired trajectory, and $y(z)$ is the system output. For implementation, equation (5) will be converted to a difference equation similar in form to equation (2). Pole placement design uses the system parameters to calculate the coefficients of the polynomials to achieve a desired closed-loop system response. In this study, the controller polynomials are chosen to provide a pole placement controller with integral action. Pole placement is considered a modern approach to controller design. It is a linear controller and requires accurate knowledge of open-loop system dynamics to achieve precise placement of the closed-loop system poles. It has a distinct advantage in that tuning the controller is not a trial-and-error process but a well-defined, mathematical approach using a desired closed-loop system response chosen by the designer. In the practical case, where the open-loop system dynamics are reasonably known, a controller design that closely meets the desired closed-loop response can be achieved easily and very quickly.

The continuous-time transfer function of the motor-driven vertical stage is

$$G(s) = \frac{q(s)}{T_E(s) - T_L(s)} = \frac{1216.448}{s(s + 5.324098 \times 10^{-5})} . \quad (6)$$

The z -transform of $G(s)$ for a sampling period of 0.005 s (200-Hz rate) is

$$G(z) = \frac{0.0152056(z+1)}{z^2 - 2z + 1} = \frac{b_0(z+1)}{z^2 - a_1z + a_2} . \quad (7)$$

For this system, the parameters in the numerator are equivalent and are represented by one parameter, b_0 , rather than two. The desired transfer function for the closed-loop system is chosen to be

$$\frac{Bm(z)}{Am(z)} = \frac{\beta 0.0152056(z+1)}{z^2 - 1.84291z + 0.852144} , \quad (8)$$

where β is chosen to give the unit steady state gain. The characteristic equation (denominator) of the desired closed-loop system provides a second-order response with a natural frequency of 10 rad/s and a relative damping of 0.8. The interested reader is referred to Astrom and Wittenmark² for derivation of the controller polynomials. The controller polynomials are functions of the system parameters b_0 , a_1 , and a_2 in equation (7). The STC must estimate these parameters in order to calculate the control gains while also controlling the system.

5. EXPERIMENTS

5.1 Comparison of Proportional-Integral-Derivative and Adaptive Exact Model Knowledge Controller

For the first set of experiments comparing the PID and the adaptive EMK controller, the sample period is chosen to be 0.0005 s, which gives a sample rate of 2,000 Hz. The PID controller gains are obtained by trial-and-error technique, as the Zeigler-Nichols tuning method and other “canned” tuning methods³ produce gains that are too conservative to take advantage of the performance capabilities of the motor-driven linear stage in the test platform. The gains selected are $K_P = 15.7$, $K_I = 0.002$, and $K_D = 0.08$.

The performance of the PID controller is illustrated in figures 3 and 4. In each case, the controller is presented with the desired trajectory that is described by the following equation, which provides a trajectory in units of millimeters:

$$r(t) = 25.0 \sin(2\pi t) (1 - e^{-0.3t^3}) . \quad (9)$$

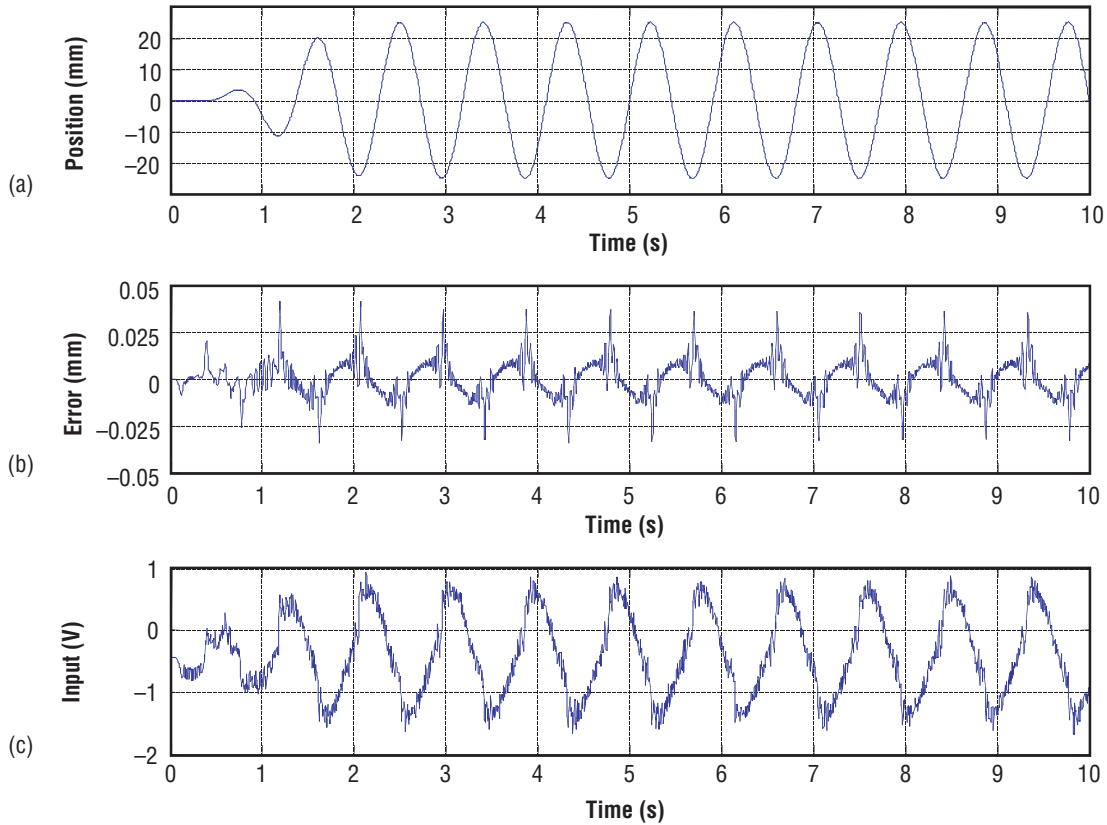


Figure 3. PID controller response with 27-lb load for (a) position, (b) error, and (c) input.

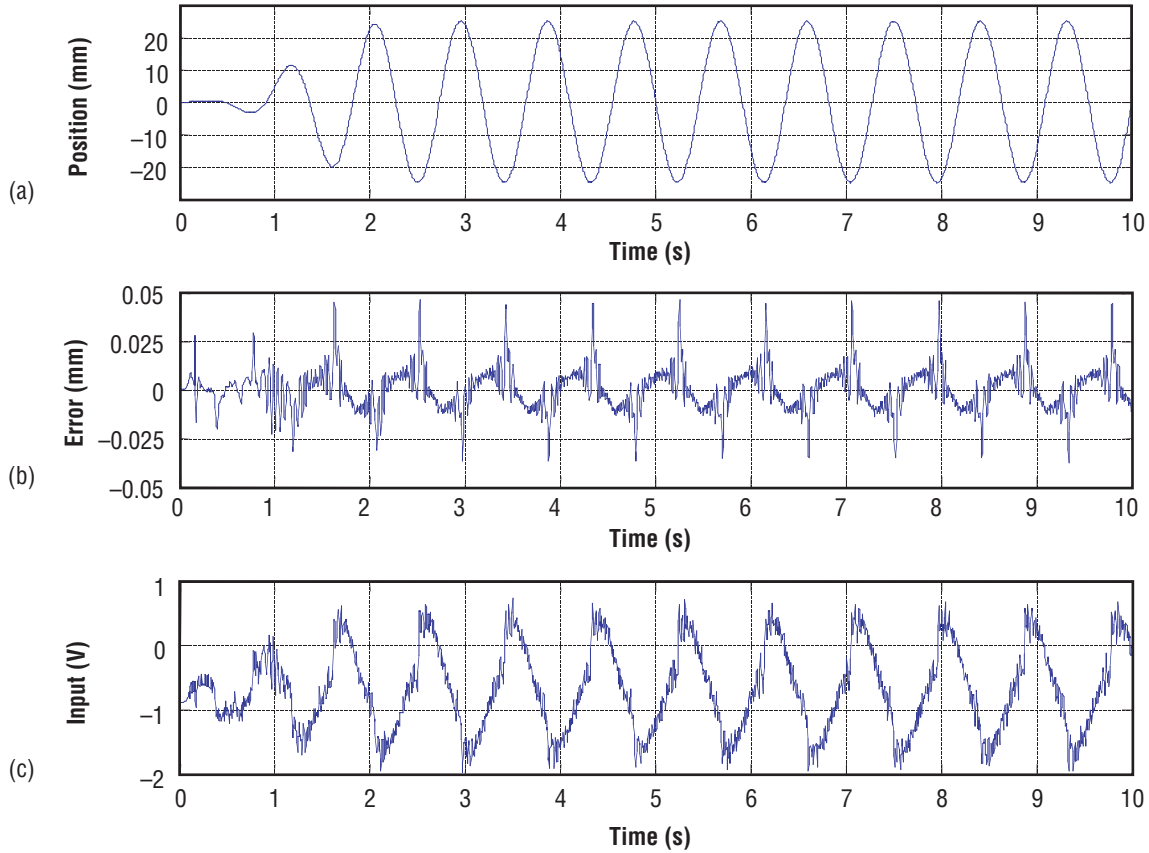


Figure 4. PID controller response with 50-lb load for (a) position, (b) error, and (c) input.

In the firmware, an approximation to π is used, so the frequency of the sine wave is not exactly 1 Hz (2π rad/s). Figure 3 shows the performance of the system with a load of 27 lb placed on the carriage of the vertical stage. The error between position of the carriage and the desired trajectory is small relative to the magnitude of the desired trajectory; figure 3(a) shows only the carriage position. If the desired trajectory were plotted with the position on this graph, the position would appear to have no tracking error relative to the desired trajectory. Figure 3(b) shows the tracking error and 3(c) shows the control input to the vertical stage drive. In this system, the control input is a voltage command with a range of ± 10 V. This voltage command represents a torque command for the motor. Figure 4 shows the performance of the system with a 50-lb load placed on the carriage. Note that there is a visible increase in the tracking error. Table 1 presents the mean, standard deviation, and maximum absolute magnitude of the tracking error at steady state. The maximum magnitude of the tracking error increases by 28.8 percent with the increase in load.

Table 1. PID control tracking error metrics.

	27-lb Load	50-lb Load
Mean (mm)	-5.186×10^{-4}	5.2131×10^{-4}
Standard deviation (mm)	0.0102	0.0113
Maximum magnitude (mm)	0.0361	0.0465

The PID controller provides good response without utilizing any knowledge of the system dynamics. However, an adaptive controller can estimate the parameters of the system dynamics and use these to automatically tune a controller.

For comparison of performance with the PID controller, the adaptive EMK controller is given the same desired trajectory defined by equation (9). The sampling period is 0.0005 s, $K_S = 0.18$, and $\alpha = 100$. The tracking error for the adaptive EMK controller is presented in figure 5. Figure 5(a) presents the tracking error for a 27-lb load and 5(b) presents the tracking error for a 50-lb load. Table 2 presents the mean, standard deviation, and maximum magnitude of the tracking error at steady state. Note that the adaptive EMK controller keeps the tracking error fairly constant between the two different loads. There is no significant increase in the maximum magnitude of the error with the increased load, as there was with the PID controller. Also, the maximum absolute magnitude of the adaptive EMK controller error for both load cases is lower than that shown in table 1 for the PID controller at the 27-lb load. The increase in the magnitude of the mean value of the error for the 50-lb load in table 2 is not considered detrimental, because the positive and negative error magnitudes are not symmetric for this case, as shown in figure 5(b). Actually, this is an artifact of the improved control performance because the maximum positive magnitude of the error is on the order of 0.02. This is roughly 30 percent less than the absolute maximum magnitude listed in table 2. This shows the limitations of using statistical measures based on the assumption of Gaussian distribution. While the increase in magnitude of the mean error value taken by itself seems to indicate poorer control performance, inspection of the plot in figure 5(b) reveals this to be due to the obviously non-Gaussian distribution of the error values.

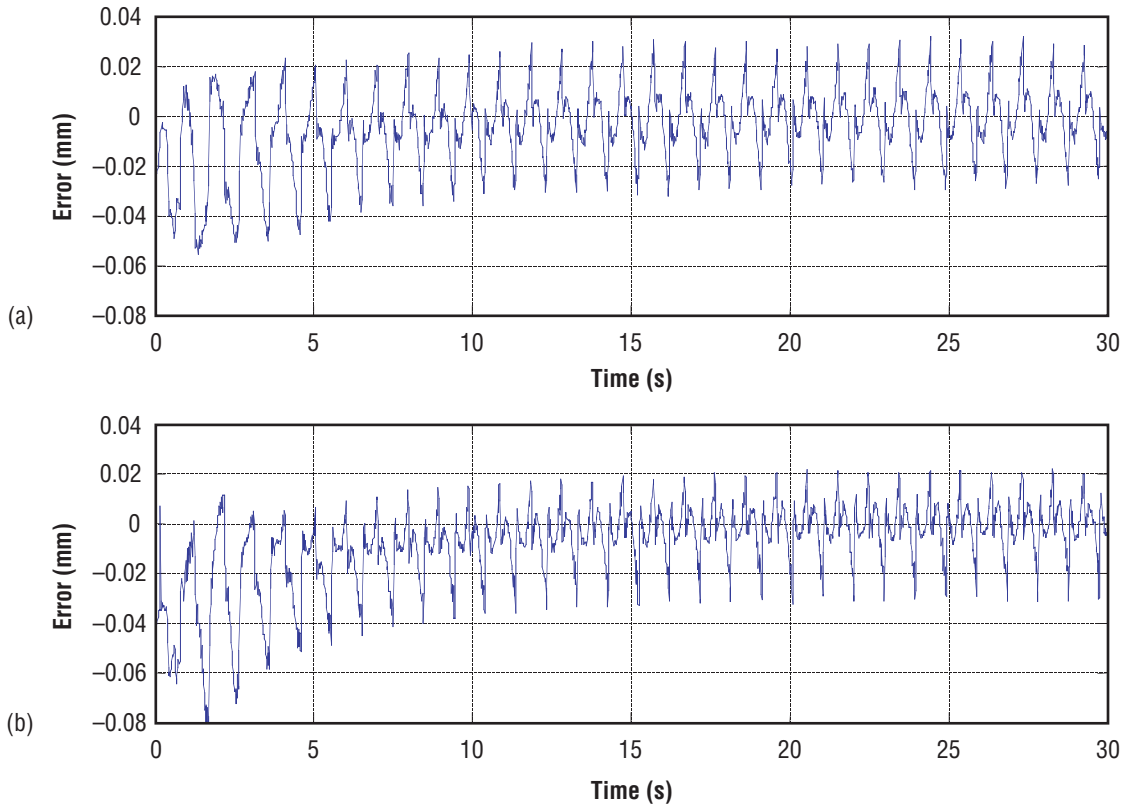


Figure 5. Adaptive EMK controller error response with (a) 27-lb load and (b) 50-lb load.

Table 2. Adaptive EMK control tracking error metrics.

	27-lb Load	50-lb Load
Mean (mm)	-8.9135×10^{-4}	-13×10^{-4}
Standard deviation (mm)	0.0125	0.01
Maximum magnitude (mm)	0.0325	0.0331

The estimates of the system inertia, damping, and load torque are shown in figures 6 and 7 for the two different cases of the 27- and 50-lb load on the carriage. Calculated values for the inertia, damping, and load torque based on manufacturer's data and the 27-lb load are inertia, $J = 0.0269039$ oz-in-s²; damping, $B = 1.4324 \times 10^{-6}$ oz-in-s, load torque, $T_L = -17.06848$ oz-in.

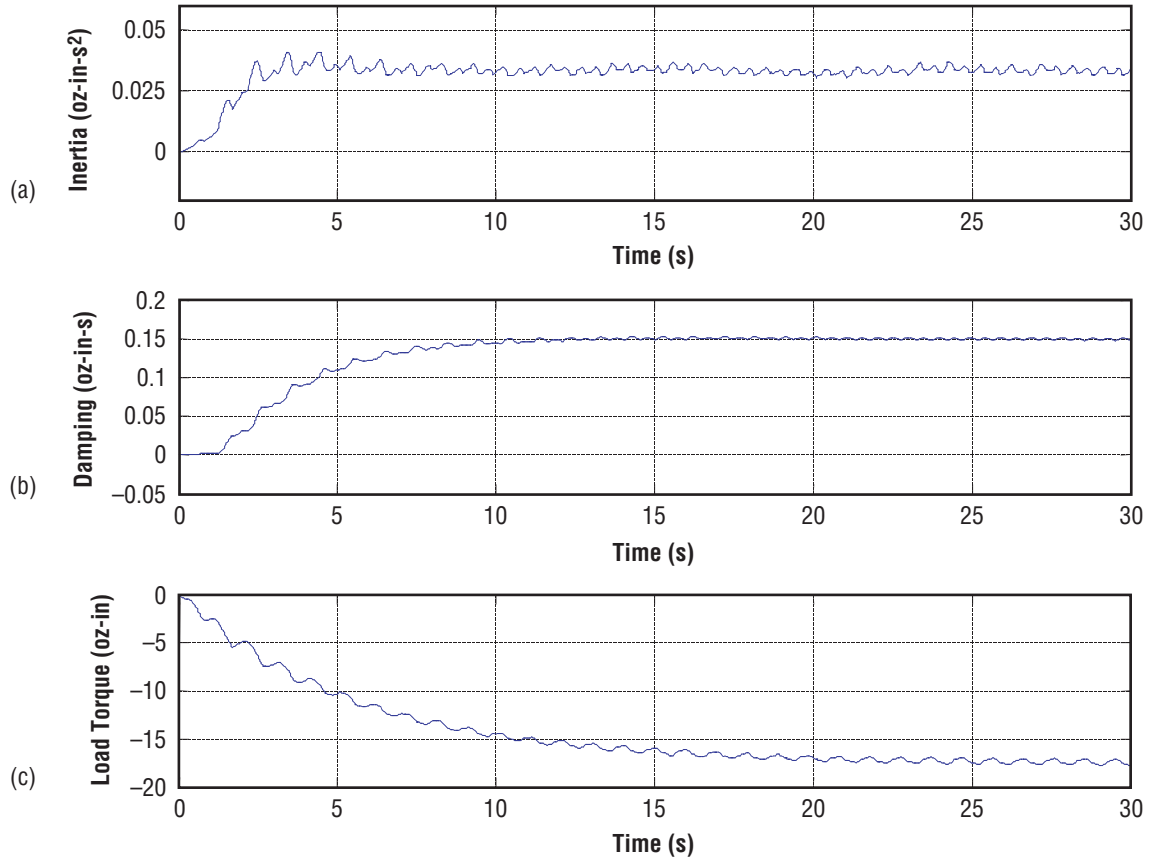


Figure 6. Parameters estimated by the adaptive EMK controller for 27-lb load for (a) inertia, (b) damping, and (c) load torque.

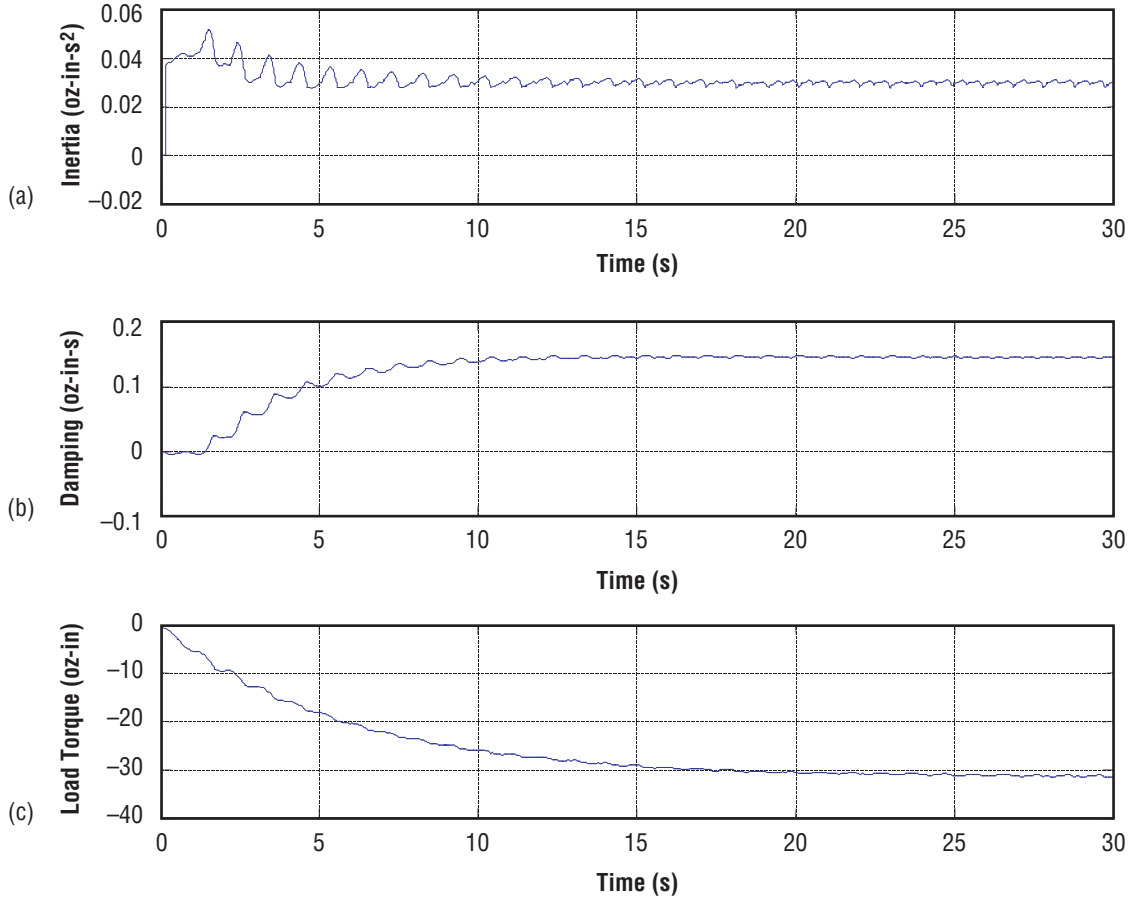


Figure 7. Parameters estimated by the adaptive EMK controller for 50-lb load for (a) inertia, (b) damping, and (c) load torque.

The negative value of the load torque is due to the direction of motor shaft rotation required to oppose gravity. In figure 6, the estimated inertia is on the order of 0.03 oz-in-s^2 , and the estimated torque load is on the order of -17 oz-in . Both are close to the calculated values. But the damping is on the order of 0.15 oz-in-s , indicating that there is considerably more damping in the system than can be accurately calculated using system specifications obtained from the manufacturer. The adaptive EMK controller is able to determine the true damping from the system response. In figure 7, the load is increased to 50 lb and the estimated load torque nearly doubles to a value of approximately -32 oz-in , as would be expected with a 185-percent increase in load on the stage carriage. The estimated inertia and damping in figure 8 closely match the values estimated for the 27-lb load. While the load on the carriage is a factor in the total inertia of the system, the rotor inertia of the motor and the inertia of the stage lead screw dominate the total inertia.

The adaptive EMK controller input to the stage drive is shown for the 50-lb load case in figure 8. Comparing this to the input produced by the PID controller for the 50-lb case shows no reduction in control effort by the adaptive EMK controller. The adaptive EMK controller produces commands with increased maximum absolute magnitude. This can be observed easily by comparing figure 4(c) with figure 8.

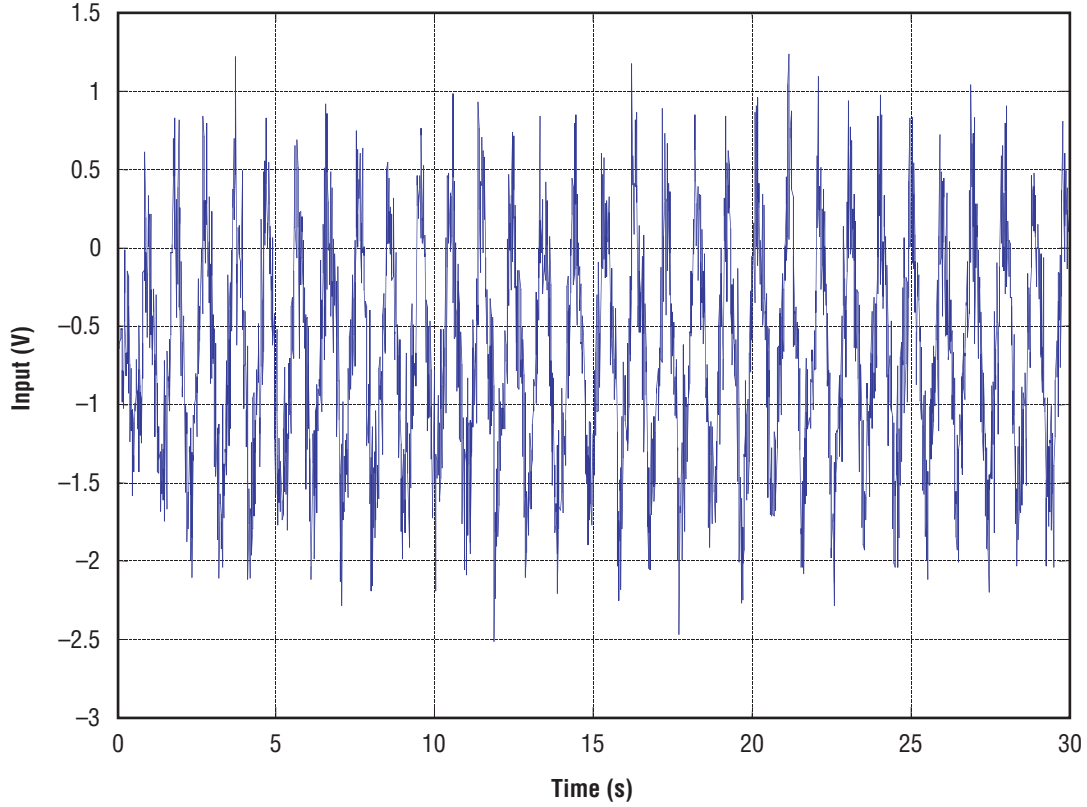


Figure 8. Adaptive EMK control input to the translation stage with 50-lb load.

The literature indicates that the adaptive EMK controller can provide an order of magnitude reduction in tracking error magnitude and significant reduction in control effort when compared with the performance of a linear PD controller. Dawson et al.¹ used a test platform consisting of a one-link robot arm. In this case, the load torque is nonlinear with respect to angular position. In the case of the motor-driven vertical stage, changing the weights on the stage carriage can vary the torque load, but it is only bias, as it remains constant regardless of stage position. This implies that the adaptive EMK controller should provide much better results in a dynamic system with nonlinearities. Additionally, Dawson et al. recommend including the motor and drive electrical dynamics in the controller design. The rationale is that these dynamics effectively filter out higher order frequency content in the controller input signal and therefore should not be neglected by using an inner, high-gain torque (current) control loop, as is used in this investigation. Including these dynamics is said to improve position tracking performance. This is a topic for future study, as Dawson et al. used linear voltage amplifiers to drive the motor in their study. Most practical motor-driven systems use motor drives consisting of H-bridges of power transistors, switched on and off by pulse width modulated command signals. This is the type of motor drive used in this study. Linear amplifier dynamics are considerably easier to model accurately than those of switched transistor drives.

5.2 Comparison of Pole Placement and Self-Tuning Controllers

For this experiment, the sampling period is 0.005 s (200-Hz rate), and a_1 and a_2 are initially set to 0, while b_0 is initially set to 0.001. Figure 9 shows the online estimation of the system parameters, while figure 10 illustrates the control system response to a desired trajectory consisting of a 0.25-Hz square wave with 25-mm amplitude. The STC rapidly converges to an approximate solution and provides good control response. The STC estimates for the system parameters are $b_0 = 0.0109328$, $a_1 = -1.9771677$, and $a_2 = 0.976626$.

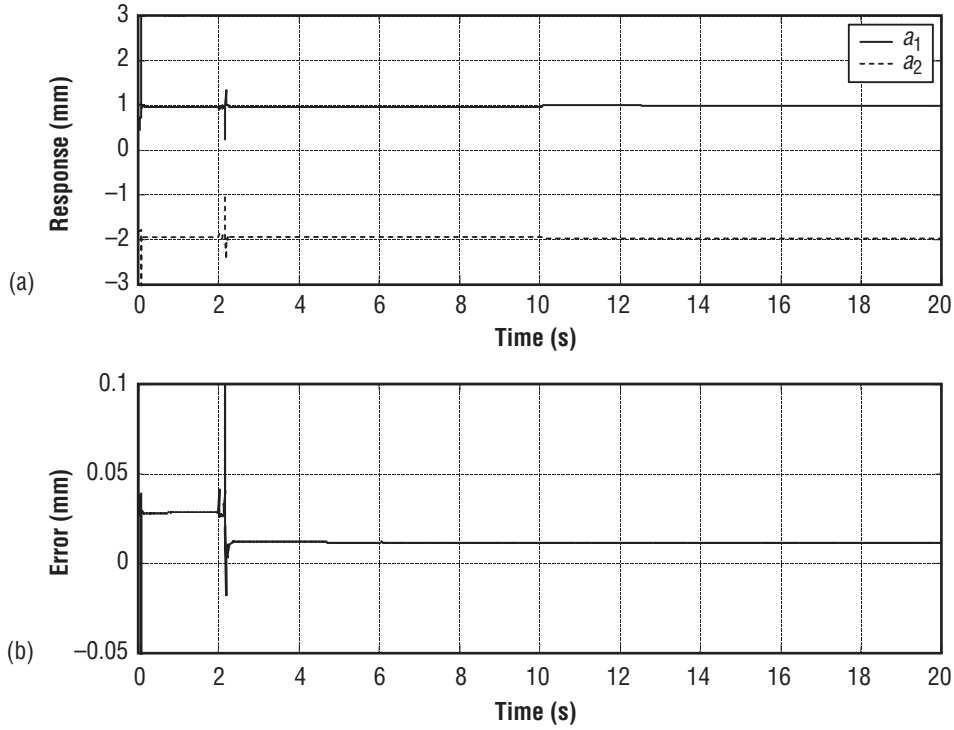


Figure 9. Online estimation of system parameters by STC for (a) a_1 and a_2 and (b) b_0 .

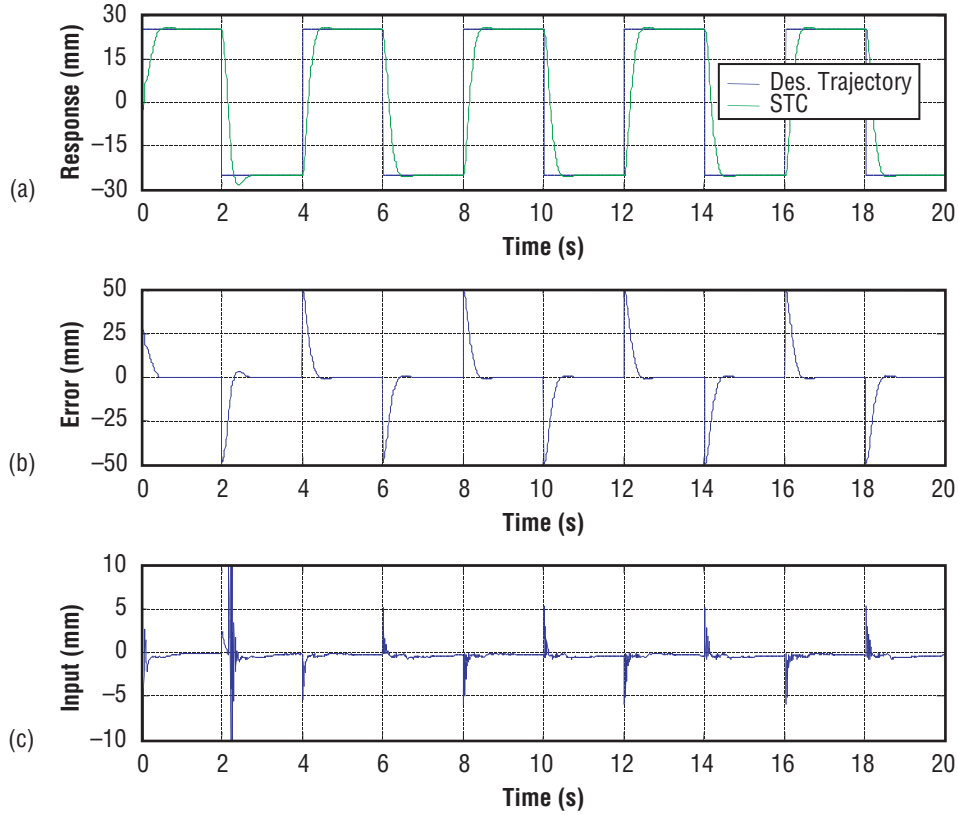


Figure 10. STC performance with 27-lb load for (a) position response to desired position trajectory, (b) error, and (c) input.

Despite the differences between the calculated values in equation (7) and the estimates, the resulting pole placement controller performs very well. It is worth noting that using the damping (0.15 oz-in-s) and inertia (0.03 oz-in-s²) estimated by the adaptive EMK controller gives a discrete time system with the following parameters: $b_0 = 0.0135234$, $b_1 = 0.01341112$, $a_1 = -1.97531$, and $a_2 = 0.97531$.

These “new” values of a_1 and a_2 are closer to the estimated values obtained by the STC, once again indicating that an adaptive controller can estimate the “true” parameters of a system. The denominator of the motor-driven vertical stage transfer function contains the damping parameter and the inertia parameter. However, the numerator now has two parameters, and $b_1 \neq b_0$. These “new” numerator parameters are nearly equivalent and can be represented by one parameter in practice. The estimated value of b_0 implies that there is lower gain in the motor-driven vertical stage than that calculated from system specifications.

Plots are given in figure 11 comparing the response of the STC to the response of the pole placement controller designed using the exact values of the system parameters in equation (7). Note that after the STC parameter estimates converge, the two controllers provide very similar steady state response with the exception of small errors during the transitions between the positive and negative 25-mm commands. At steady state, both controllers provide position responses that are within ± 0.030 mm

of the desired trajectory. Use of the STC has the clear advantage of being able to tune itself in a matter of seconds. In comparison with the typical manual trial-and-error approach to tuning a PID controller, the tuning process for the STC is much faster and automatically adapts to any changes in the parameters of the system being controlled while providing acceptable control prior to convergence of the estimates.

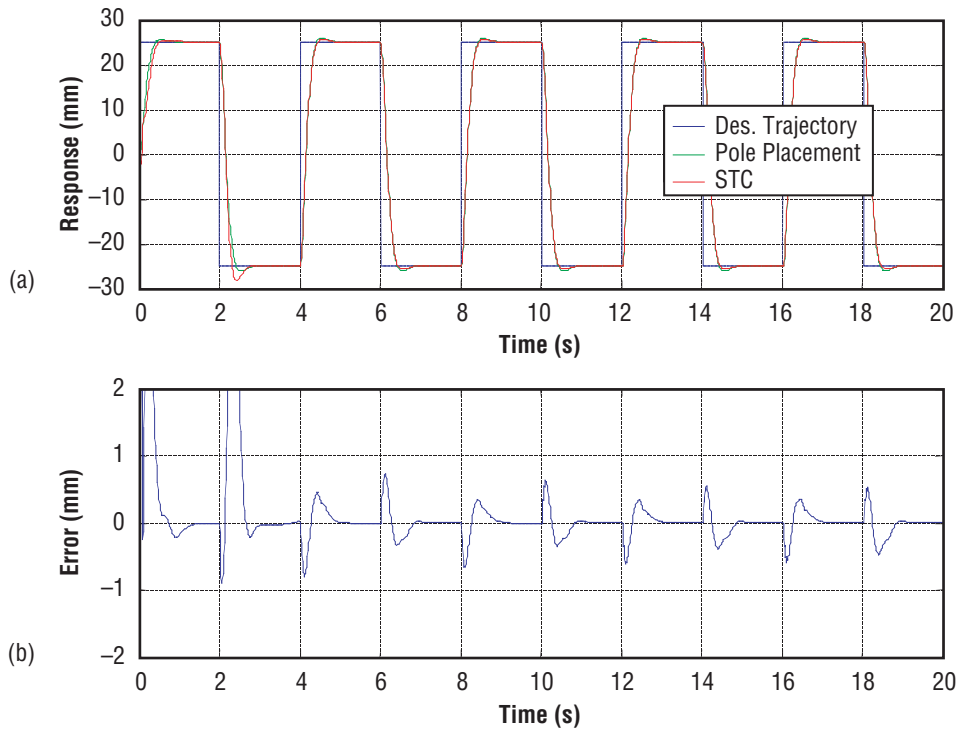


Figure 11. Comparison of STC and standard pole placement control for (a) position response and (b) error.

6. SUMMARY

In this investigation, it is shown that adaptive controllers have significant advantages over linear controllers with fixed gains. Adaptive control provides improved control system performance in the face of unanticipated changes in actuator mechanical system dynamics. It can also provide improved actuator performance due to adaptation to unmodeled dynamic system parameter variation and inaccurate parameter characterization. The ability to self tune while controlling the system is an advantage that can be utilized to improve the capabilities of spacecraft of various types. This can provide rapid control loop tuning at the commissioning and recertification of reusable spacecraft subsystems on the ground. Deep space experiments and spacecraft can self tune when required and adapt to changes in system dynamics that would otherwise degrade the performance of actuator controls. Adaptive control has the capability to accommodate limited system faults which do not prevent actuator motion and to provide fault detection. Limited faults, such as an increase in friction, can be accommodated without failure through adaptation of controller gains. Hard failures, such as a break in mechanical linkage, cannot be accommodated. The system will fail, but changes in the dynamics can be detected and reported to a higher level controller. Future work will include the refinement of the adaptive control approaches to allow deployment of these, or similar adaptive controllers, at the actuator level in spacecraft.

REFERENCES

1. Dawson, D.M.; Hu, J.; and Burg, T.C.: *Nonlinear Control of Electric Machinery*, Marcel Dekker, Inc., San Diego, CA, pp. 99–129, 1998.
2. Astrom, K.J.; and Wittenmark, B.: *Adaptive Control*, 2d ed., Addison-Wesley Publishing Company, Inc., New York, NY, pp. 77–101, 1995.
3. Ellis, G.: *Control System Design Guide*, Academic Press, Reading, MA, pp. 41–135, 2000.

REPORT DOCUMENTATION PAGE			Form Approved OMB No. 0704-0188	
Public reporting burden for this collection of information is estimated to average 1 hour per response, including the time for reviewing instructions, searching existing data sources, gathering and maintaining the data needed, and completing and reviewing the collection of information. Send comments regarding this burden estimate or any other aspect of this collection of information, including suggestions for reducing this burden, to Washington Headquarters Services, Directorate for Information Operation and Reports, 1215 Jefferson Davis Highway, Suite 1204, Arlington, VA 22202-4302, and to the Office of Management and Budget, Paperwork Reduction Project (0704-0188), Washington, DC 20503				
1. AGENCY USE ONLY (Leave Blank)		2. REPORT DATE August 2002		3. REPORT TYPE AND DATES COVERED Technical Memorandum
4. TITLE AND SUBTITLE Test Platform for Advanced Digital Control of Brushless DC Motors (MSFC Center Director's Discretionary Fund Final Report, Project No. 00-04)			5. FUNDING NUMBERS	
6. AUTHORS D.A. Gwaltney				
7. PERFORMING ORGANIZATION NAME(S) AND ADDRESS(ES) George C. Marshall Space Flight Center Marshall Space Flight Center, AL 35812			8. PERFORMING ORGANIZATION REPORT NUMBER M-1055	
9. SPONSORING/MONITORING AGENCY NAME(S) AND ADDRESS(ES) National Aeronautics and Space Administration Washington, DC 20546-0001			10. SPONSORING/MONITORING AGENCY REPORT NUMBER NASA/TM-2002-211917	
11. SUPPLEMENTARY NOTES Prepared by Avionics Department, Engineering Directorate				
12a. DISTRIBUTION/AVAILABILITY STATEMENT Unclassified-Unlimited Subject Category 33 Nonstandard Distribution			12b. DISTRIBUTION CODE	
13. ABSTRACT (Maximum 200 words) A FY 2001 Center Director's Discretionary Fund task to develop a test platform for the development, implementation, and evaluation of adaptive and other advanced control techniques for brushless DC (BLDC) motor-driven mechanisms is described. Important applications for BLDC motor-driven mechanisms are the translation of specimens in microgravity experiments and electromechanical actuation of nozzle and fuel valves in propulsion systems. Motor-driven aerocontrol surfaces are also being utilized in developmental X vehicles. The experimental test platform employs a linear translation stage that is mounted vertically and driven by a BLDC motor. Control approaches are implemented on a digital signal processor-based controller for real-time, closed-loop control of the stage carriage position. The goal of the effort is to explore the application of advanced control approaches that can enhance the performance of a motor-driven actuator over the performance obtained using linear control approaches with fixed gains. Adaptive controllers utilizing an exact model knowledge controller and a self-tuning controller are implemented and the control system performance is illustrated through the presentation of experimental results.				
14. SUBJECT TERMS adaptive control, PID control, digital control, brushless DC motor, BLDC motor, self tuning, parameter estimation, embedded, actuator			15. NUMBER OF PAGES 28	
			16. PRICE CODE	
17. SECURITY CLASSIFICATION OF REPORT Unclassified	18. SECURITY CLASSIFICATION OF THIS PAGE Unclassified	19. SECURITY CLASSIFICATION OF ABSTRACT Unclassified	20. LIMITATION OF ABSTRACT Unlimited	